Fabrication of high-aspect ratio, micro-fluidic channels and tunnels using femtosecond laser pulses and chemical etching

Yves Bellouard
Center for Automation Technologies, Rensselaer Polytechnic Institute
CII 8211, 110 8th Street, Troy, New York 12180-3590
bellouard@cat.rpi.edu

Ali Said, Mark Dugan, and Philippe Bado
Translume Inc., 755, Phoenix Drive, Ann Arbor, Michigan 48108-2222

Abstract: We present novel results obtained in the fabrication of high-aspect ratio micro-fluidic microstructures chemically etched from fused silica substrates locally exposed to femtosecond laser radiation. A volume sampling method to generate three-dimensional patterns is proposed and a systematic SEM-based analysis of the microstructure is presented. The results obtained gives new insights toward a better understanding of the femtosecond laser interaction with fused silica glass (a-SiO_2).

OCIS codes: (140.7090) Ultrafast lasers; (160.2750) Glass and other amorphous materials; (320.2250) femtosecond phenomena; (320.7130) Ultrafast processes in condensed matter, including semiconductors.

References and Links

1. Y. Kondo, T. Suzuki, H. Inouye, K. Miura, T. Mitsuyu, and K. Hirao, "Three-Dimensional Microscopic Crystallization in Photosensitive Glass by Femtosecond Laser Pulses at Nonresonant Wavelength," Jpn. J. Appl. Phys. **37**, L94 - L96 (1998).
2. A. Marcinkevičius, S. Juodkazis, M. Watanabe, M. Miwa, S. Matsuo, H. Misawa, and J. Nishii, "Femtosecond Laser-assisted three-dimensional microfabrication in silica," Opt. Lett. **26**, 277-279 (2001).
3. K. M. Davis, K. Miura, N. Sugimoto, and K. Hirao, "Writing waveguides in glass with a femtosecond laser," Opt. Lett. **21**, 1729-1731 (1996).
4. A. Strelsov and N. Borrelli, "Study of femtosecond-laser-written waveguides in glasses," J. Opt. Soc. Am. B **19**, 2496-2504 (2002).
5. A. Agarwal and M. Tomozawa, "Correlation of silica glass properties with the infrared spectra," J. Non-Cryst. Solids **209**, 166-174 (1997).
6. R. S. Taylor, C. Hnatovsky, E. Simova, D. M. Rayner, M. Mehandale, V. R. Bhardwaj, anfd P. B. Corkum, "Ultra-high resolution index of refraction profiles of femtosecond laser modified silica structures," Opt. Express **11,** 775-781 (2003), http://www.opticsexpress.org/abstract.cfm?URI=OPEX-11-7-775.
7. Y. Bellouard, A. Said, M. Dugan, P. Bado, "Monolithic Three-Dimensional Integration of Micro-Fluidic Channels and Optical Waveguides in Fused Silica," MRS Proceedings, vol. 782, Boston 2003 (in press).
8. P. Oberson, B. Gisin, B. Huttner, and N. Gisin, "Refracted near-field measurements of refractive index and geometry of silica-on-silicon integrated optical waveguides," Appl. Opt. **37**, 7268-7272 (1998).
9. P. Bado, A. Said, M. Dugan, T. Sosnowski, and S. Wright "Dramatic improvements in waveguide manufacturing with femtosecond lasers," in NFOEC, Dallas, Sept. 2002.
10. R. Gattass, I. Maxwell, J. Ashcom, and E. Mazur, "Transition from repetitive to cumulative thermal processing in femtosecond laser induced machining of embedded waveguides" in Photonics West, Proc. SPIE **4978**, 43- (2004).
11. C. Schaffer, J. Garcia and E. Mazur "Bulk heating of transparent materials using a high repetition-rate femtosecond laser," Appl. Phys. A - Mater **76**, 351-354 (2003).
12. K. Awazu, H. Kawazoe, "Strained Si – O – Si bonds in amorphous SiO_2 materials: A family member of active centers in radio, photo, and chemical responses," J. Appl. Physics **94**, 6243-6262 (2003).
13. C. Fiori, R.A.B. Devine, "Evidence for a wide continuum of polymorphs in a-SiO_2," Phys. Rev. B **33,** 2972-2974 (1986).
14. F. L. Galeener, "Planar rings in glass," Solid State Commun. **44**, 1037-1040 (1982).

#4156- $15.00 US
Received 2 April 2004; revised 29 April 2004; accepted 30 April 2004

1. Introduction

For the past decade, Lab-on-a-Chips and Biochips have generated increasing attention as a means to foster new drug development, faster bio-analysis and rational natural resource usage. Among materials considered for these applications, amorphous fused silica is particularly attractive. It exhibits good optical properties from the UV to the IR and has excellent chemical stability.

In this paper, we report on a fabrication process based on femtosecond laser exposure and chemical etching to manufacture micro-fluidic channels of arbitrary size and shape in fused silica substrates. We also present a detailed analysis of the etching process based on SEM-observations that gives insight toward a better understanding of the femtosecond laser interaction with amorphous fused silica. We also propose a simple phenomenological model of the mechanism that leads to faster etching rates.

Kondo *et al.* [1] reported on a process based on the use of femtosecond lasers and chemical etching to fabricate micro-tunnels in photo-etchable glass. Marcinkevičius *et al.* [2] applied a similar process to manufacture micro-holes in fused silica. Although, these pioneering works have demonstrated the feasibility of the process, unresolved issues remain. The mechanism responsible for the increased etching rate has yet to be understood. It is not known if the etching mechanism is preferentially driven by the increase level of internal stress resulting from the laser exposure, the presence of voids or micro-cracks, or a laser-induced densification effect. Further the ability to generate arbitrary shapes has – so far – been limited by the laser beam shape.

We have used the process demonstrated in [1,2] combined with a volume sampling technique to fabricate fluidic channels and tunnels of virtually any shapes. This volume sampling technique consists in stacking and arranging Laser-Affected-Zone (LAZ) units to define the volume to be etched. To be effective this method requires a good understanding of the effect of femtosecond laser on amorphous fused silica and in particular an understanding on how contiguous LAZ interact with each other.

Femtosecond-laser irradiation of fused silica produces two previously documented material changes: an increase of the refractive index [3,4] and an increase of the etching rate [2]. The understanding of observed effects is subject to discussion (see for instance [4] concerning refractive index change). Agarwal *et al.* [5] have shown that a change of the Si – O – Si bond angle can be correlated to a variety of glass properties such as the etching rate, the density, induced-stress and the refractive index. Taylor *et al.* [6] have shown that the etch rate of femtosecond laser modified silica structures is approximately linearly dependent on the induced index of refraction change, at least up to index changes of 1 percent. Therefore, this study is not only interesting for the development of this micro-fabrication process but also to better understand the overall effect of femtosecond laser radiation on fused silica.

2. Experimental method

2.1 Volume sampling

When fused silica is exposed to femtosecond laser pulses, the index of refraction is locally modified along an ellipsoid-like shape whose volume is defined by the optical system and by the laser parameters (beam waist, energy, etc.). Based on what is known about the effect of density on index of refraction and the effect of pressure on the etching rate [3-7], we assume that there exists a direct spatial correlation between the zone where the index of refraction has been changed and the zone that will have a higher etching rate. Therefore, we have considered an index map produced by refractive near field profilometry [8,9] as a measure of the unit Laser Affected Zone (unit-LAZ) that defines the volume element to be etched.

Figure 1 shows an illustration of the volume sampling and an example of the index map. Since the writing speed is significantly smaller than the pulse repetition rate, juxtaposed laser-affected zones can be considered as lines in the scanning direction (Y-axis). Lines parallel to each other define a matrix in the transverse (X, Z) plane (Fig. 1).

#4156- $15.00 US Received 2 April 2004; revised 29 April 2004; accepted 30 April 2004

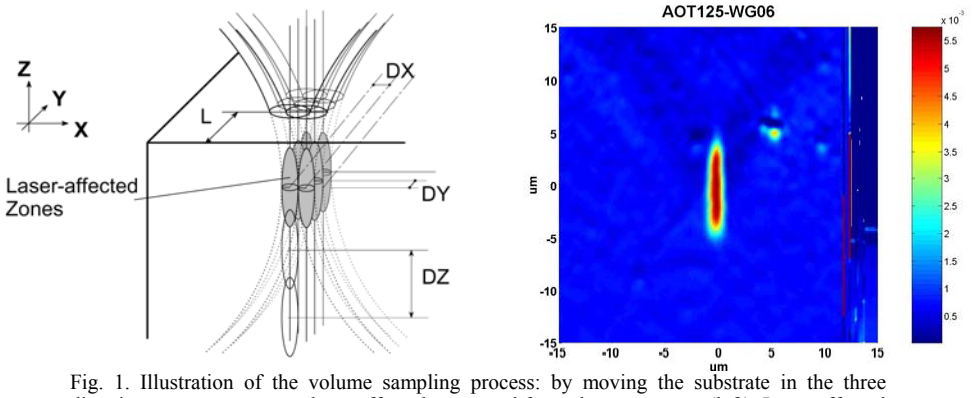

Fig. 1. Illustration of the volume sampling process: by moving the substrate in the three directions, one can connect laser-affected zones and forms larger patterns (left). Laser-affected zones (LAZ) are represented by an ellipsoid and since fs-laser matter interaction involved non-linear process, the ellipsoid short axis can be smaller than the spot-size itself. The volume to be etched is sampled by connecting discrete unit-LAZ zones. Right: a typical refractive index map obtained after femtosecond laser exposure of a single line. This pattern was taken as a reference to define the shape and size of a unit-LAZ. The map was obtained using a refractive near-field profilometer.

This volume sampling is somewhat similar to the pattern generation in stereolithography process except that in our case, we define the volume to be removed.

2.2 Process description

A two-step procedure was applied:

1. **Laser exposure:** the desired pattern of a tunnel or channel is applied to the glass by writing adjacent lines (volume sampling). To do so, the substrate is mounted on motorized translation stages with a typical repeatability of 300 nm and a resolution of 100 nm. The sample is exposed to femtosecond laser pulses emitted from a Ti:Sapphire laser operating at 800 nm. The pulse width is 100-fs, and the repetition rate is set at 250 kHz. The linear spot size is approximately 1 μm. Note that femtosecond -illumination of fused silica is a multi-photon process, thus the linear spot size may not be the relevant dimension. Further nonlinear effects may make the LAZ non-symmetrical along the Z-axis (as defined in Fig. 1). The average power ranges from 20 to 400 mW, which corresponds to pulse energies ranging from 55-nJ to 1 microjoule. Writing speed along the Y-axis ranges from 100 to 500 μm/sec. The overlap between laser-affected zones is significant along the Y-axis. Affected regions are hit multiple times by the laser (500 to 2500 times). However, considering the relatively low repetition rate of the laser, there is no significant residual heating from one pulse to the next [10,11].
2. **Etching:** After the laser exposure, the fused silica is immersed in a low-concentration aqueous solution of HF acid for three hours. Ambient temperature solutions with concentration of 2.5 to 5 % were used. The volume of the solution is typically 40 ml (or at least ten times the volume of the glass specimen). After etching, specimens are rinsed in de-ionized water and cleaned in an ultrasonic bath made of isopropanol-3 solution for about 5 min. The etched samples are rinsed multiple times.

High purity fused silica substrates (Dynasil 1100) were used. This glass is characterized by a typical OH content in the range of 600-1000 ppm, a Cl content of 90 ppm and a total metallic impurities content 1-2 ppm. An optical microscope equipped with high precision motorized stages was used to visually inspect and measure tunnel and surface channel profiles. Etched zones are clearly visible and have a characteristic opaque or dark color in bright field and are shiny in dark field. A conventional Scanning Electron Microscope and a Field Emission were also used to inspect specimens at higher magnifications.

#4156- $15.00 US Received 2 April 2004; revised 29 April 2004; accepted 30 April 2004

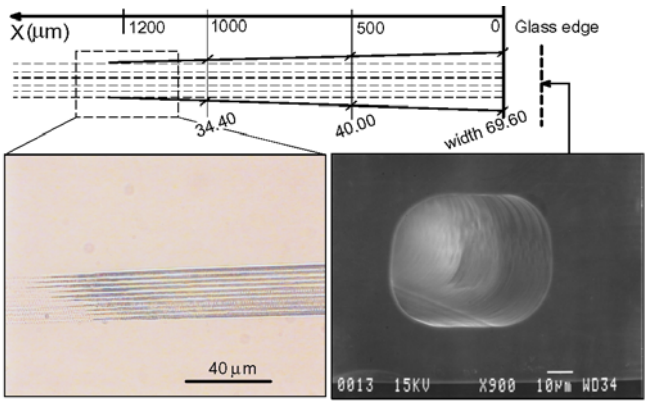

Fig. 2. Micro-tunnel: optical and scanning electron microscopes observations [7]. The width (in µm), measured along the tunnel length, is indicated in italic on the schematic diagram of the tunnel.

3. Experimental results

3.1 Tunnels

Channels and tunnels were made using the experimental procedure described above. Initial results have been reported in [7]. Tunnel patterns 5 mm long were made by scanning 10 adjacent lines, equally distributed, at a speed of 100 µm/s and pulse energies of 135 nJ. The lines are spaced by 3 µm. Two different sets of tunnel patterns were considered. The first one ("tunnel-A" type) was written at a distance of 75 µm from the substrate surface facing the laser beam while the second set ("tunnel-B" type) was written deeper, at a distance of 420 µm from the same surface. For the latter, the power was slightly adjusted in order to compensate for optical aberration associated with the additional depth. The fused silica substrate containing both types of tunnels was immersed for three hours in a 5% HF solution. 1.2 mm-deep tunnels were obtained for tunnels written close to the surface (tunnels-A). A "tunnel-A" type is shown on Fig. 2. The left picture shows an optical microscope image of the tunnel extremity and the right one, a SEM picture of the tunnel entrance. The profile was measured along the tunnel length under the optical microscope. The tunnel has a slight conical structure with an angle of 2.7 deg for the first portion (0 - 0.5 mm) and 1.8 deg for the deeper portion (0.5 to 1 mm). The left picture on Fig. 2 suggests that the etching profile is propagating faster along the illuminated track. Furthermore, etching rate seems to be identical for each of the ten unit-LAZ. The length of the tunnel 1.2 mm shows that the average etching rate in the longitudinal direction, measured for a period of three hours, is in the order of 5 µm/min. In comparison, the etching rate for non-laser exposed fused silica, for the same material and under the same etching conditions, is typically 3 µm/hour [7]. Therefore, LAZ are etched about 100 times faster than non-affected regions. Figure 3 shows a partially etched tunnel that was written deeper below the glass surface (420 µm).

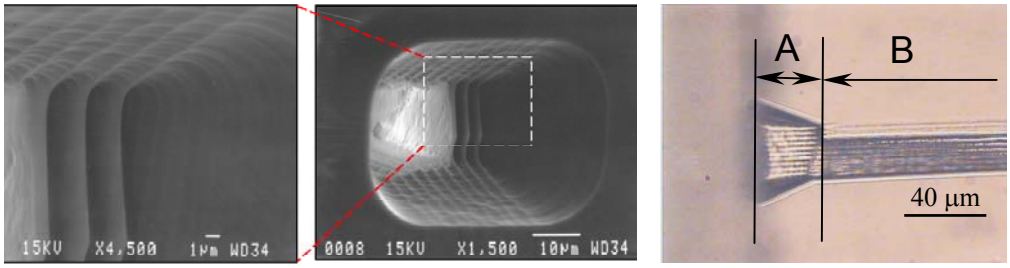

Fig. 3. SEM and optical pictures of the front end of a partially etched tunnel. The tunnel is 0.8 mm long and about 70 µm wide at the largest cross-section. Two different etching regimes (A and B) are clearly visible.

#4156- $15.00 US Received 2 April 2004; revised 29 April 2004; accepted 30 April 2004

Salient structures can be seen on Fig. 3:

- There is a conical shape at the entrance of the tunnel. We suspect this is partly a result of a clipping effect of the writing laser beam whose power gradually changes as the beam reaches the edge and goes through it. The cone shape may result from the long chemical exposure time. Two different regimes are observed: Regime A corresponds to the etching of the area affected by edge effect. Regime B seems to be very similar to the etching regime observed in completely etched tunnel. By measuring the complete length of the tunnel and assuming that the etching rate in the region B is similar to the etching rate of a uniformly etched tunnel, the etching rate in region A is typically 1 µm/min.
- An etched profile consisting of equally spaced corrugated structures is visible in the transverse direction (X-axis). Since these structures are as numerous as the initial painted lines and since the spacing is identical, we conclude a direct correlation between the written lines and the lateral etched profile. The right side of the tunnel reveals partially etched zones between lines. The regions corresponding to the center of the LAZ are etched faster than the material found in between lines.
- Noticeable, quasi-periodic oscillations in the structure of the tunnel walls (typically 1 µm) are also visible in the longitudinal direction of the channel (Y-axis). The origin of these oscillations is unknown.

3.2 Surface Channel

In a previous set of experiments [7], surface channels were made illuminating a volume consisting of a matrix of (8 x 10) lines. Matrix density parameters (dX, dZ) were chosen to be respectively 4 µm and 3 µm. It was noticed that the average etching rate (measured over a period of 3 hours) was at least in the order of 12 µm/h in the lateral and transverse corresponding to directions X and Z (Fig. 1). We have refined this data by measuring the depth profile of a deep channel after successive short etching periods of time (typ. 30 min). A 30-µm wide and 675-µm deep channel-pattern was positioned in the substrate such that the HF acid can only penetrate inside the glass through the top (Fig. 4). In this case, the pattern is made of 15 x 90 lines with a line density of 2 µm. The channel was placed enough close to the glass edge such that it is possible to measure the etched depth through direct optical observations. The measured etching speed is 1.2 µm/min.

To further investigate the etching mechanism and to reveal the patterns microstructure, systematic SEM investigations were performed on a specimen containing multiple channel-patterns written with various energy levels and etched in HF (2.5%) for two hours. Figure 5 shows channel profiles of single tracks made with increasing level of pulse energy. Those profiles were obtained by image processing (contour extraction) of optical images of single track under straight illumination.

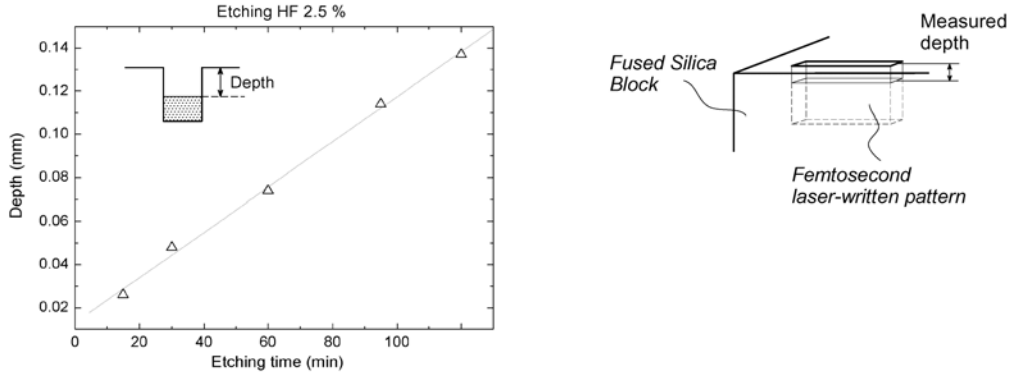

Fig. 4. Surface channel. Left – Time dependant depth etching rate. For this measurement, a micro-channel made of 15 x 90 parallel lines (30 µm wide, 675 µm deep).

#4156- $15.00 US Received 2 April 2004; revised 29 April 2004; accepted 30 April 2004

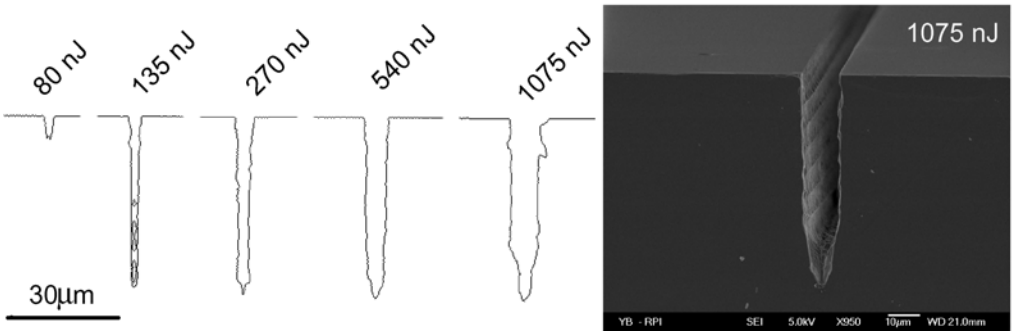

Fig. 5. Single-track channels profile. These channels were obtained by stacking lines only in the z-direction.

Eleven unit-LAZs were stacked in the z-direction (1 x 11 matrix). Increasing the pulse energy only seems to affect the width of the etched pattern. In addition, single-track channels are rather uniform and symmetric. Noticeably, the width is substantially larger than the assumed unit-LAZ.

Figure 6 shows both a picture of two completely etched channels made under the same laser writing conditions and a picture of one of the two channels taken further away from the edge. These channels are made of a matrix of 60 x 11 unit-LAZ. The length is two millimeters. Although, surface roughness is difficult to measure under SEM, we estimate typically 0.5 µm to 0.25 µm. A periodic pattern is visible on the channel walls. This periodicity corresponds to the number of unit-LAZ in the Z direction. On both sides of the channels, near the top surface, a different morphology is found over a few micrometers, suggesting a different etching regime within a few µm of the surface.

Figure 7 shows partially etched channels at three different levels of power. From left to right, the pulse energy was varying from 55 to 1075-nJ. Figure 6 left shows the typical morphology of a channel etched with pulse energy of 270-nJ. Best result in term of shape quality and etching rate are obtained for pulse energy level of 135 and 270-nJ. Surprisingly, increasing the level of pulse energy does not leave to a faster etching rate. At high pulse energy levels (>270 nJ), un-etched structures are found in the middle of the channels while the edges are fully etched.

Figure 8 shows surface topologies of the micro-channels obtained with varying pulse energy. A level of porosity of the etched surface is clearly visible for pulse energies 270 nJ, 540 nJ and 1075 nJ.

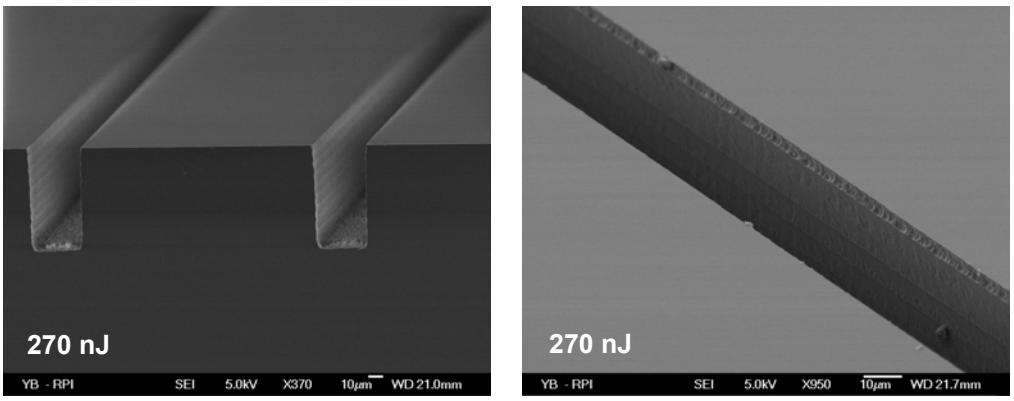

Fig. 6. Micro-channels (after 135 min): view from the glass edge (left) and further away (right).

#4156- $15.00 US Received 2 April 2004; revised 29 April 2004; accepted 30 April 2004

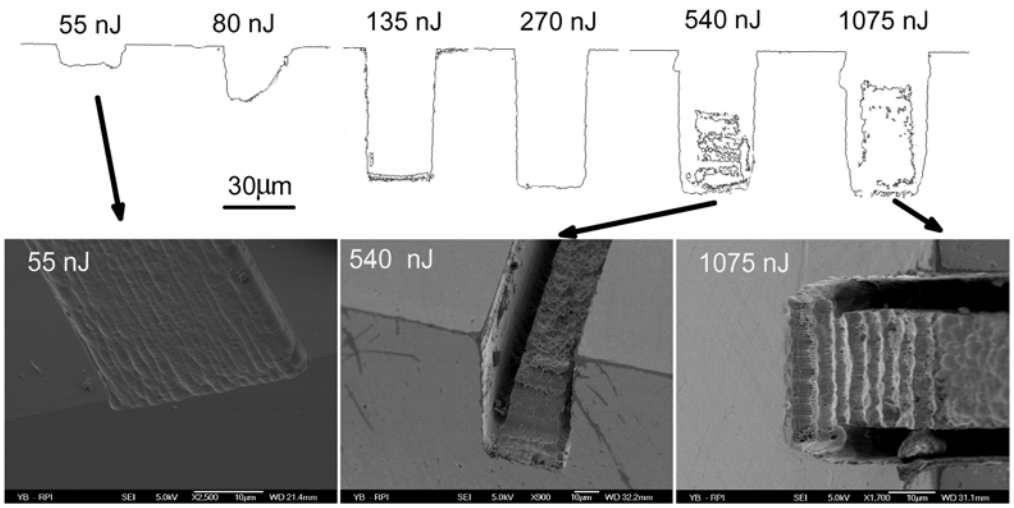

Fig. 7. Partially etched channels: three different level of power were used: from left to right: 55 (top view), 540, 1075 nJ. Number of lines is identical for the three channels.

Such pitting of the surface is not seen for the lower pulse energy. The surface morphology found in particular with channels etched with 270 and 540 nJ suggests the presence of micro-explosion sites, which surprisingly, tends to be less pronounced at higher energy.

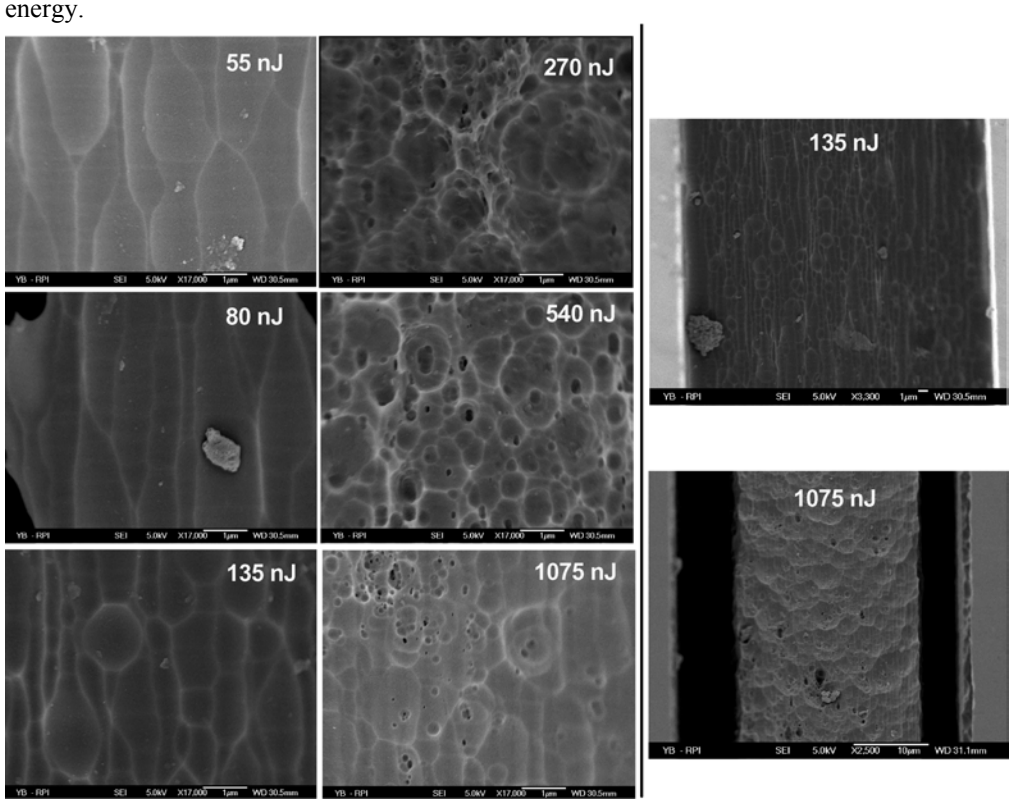

Fig. 8. (left): Surface structure of etched channels at six different level of energy. The two pictures shown on the right shows a top view of two channels. All channels were made in the same piece and with the same number of unit-LAZs.

#4156- $15.00 US
Received 2 April 2004; revised 29 April 2004; accepted 30 April 2004

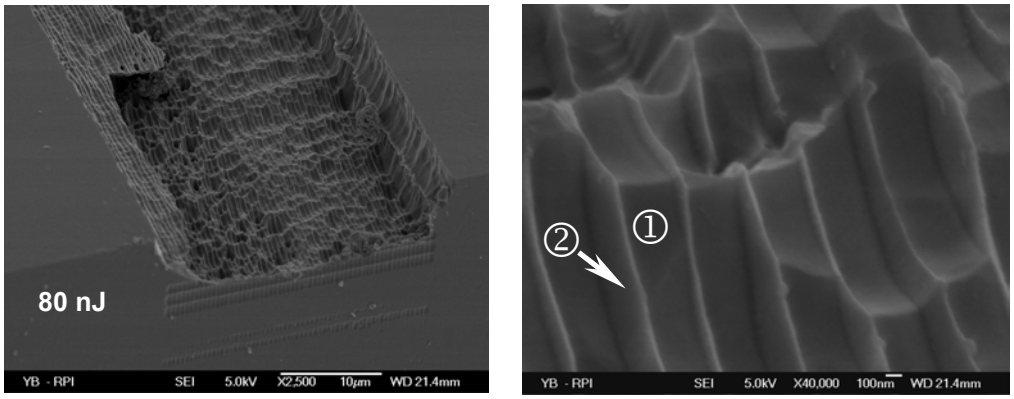

Fig. 9. A microchannel partially etched after one hour etching time. The picture on the right is a magnification of the channel central region. Distance between laser-exposed regions is 500 nm.

Figure 9 shows a channel etched for only an hour after laser exposure with a pulse energy of 80 nJ. The picture on the left is a magnification of the central portion of the channel. The etched patterns reveal different zones. These zones are labeled (1, 2). The contrast difference on the SEM image suggests a significant difference of density between the two regions and the existence of well-defined interface between the two regions that could indicate the presence of two different material phases Noticeably, the distribution of these patterns, along the lateral direction, is homogeneous and regular. The larger region (label 1) is about 400 nm wide while the smaller region (label 2) is only 100 nm wide. The shape, the periodicity and the number of those patterns link their origin to the LAZ-units patterned in the x direction.

Figure 10 shows a very deep channel (the pattern was 675 μm) that was partially etched. The pulse energy was 160 nJ and the line spacing in x was 2 μm. The etching depth reached 480 μm after two hours. Remaining material can be seen between each laser track. The thickness of this material layer is about 100 nm. The etching appears to be homogeneous across the channel width where the surface roughness near the edge is on the order of 0.25 to 0.5 μm.

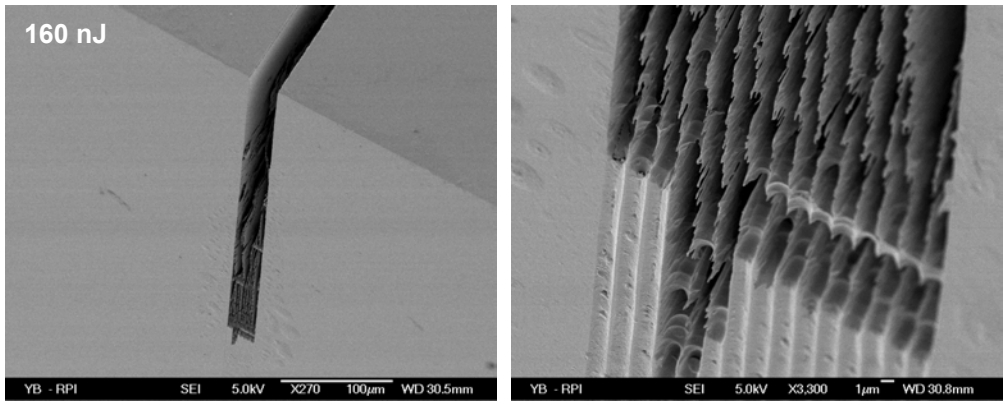

Fig. 10. Partially etched channel: distance between lines was 2 μm. The channel goes 675 μm deep. The left picture shows an overview of the partially etched channel after two hours etching time. The right picture is a magnification of the boundary between etched and un-etched zones.

#4156- $15.00 US Received 2 April 2004; revised 29 April 2004; accepted 30 April 2004

4. Discussion

From the comparison between the case of individual laser written lines and multiple laser written lines (Fig. 5 versus Fig. 6), we conclude that the presence of adjacent multiple unit-LAZ affects the etching process. Displaced unit-LAZ's (in x or z) can modify the stress field and the density profile of the individual or previously written LAZ. For all our observations, considering the pulse duration (100fs) and the repetition rate (250 kHz), we consider that thermal effects if any, are very limited in space. This argument is reinforced by observations made by others [10,11].

Single-track data indicates that the higher the laser pulse energy, the wider the laser-affected etched zone (Fig. 5). No evidence of micro-cracks is found on single-track edges and a rather homogeneous etching profile is observed along the channel depth. From these observations, we suspect the presence of internal stress surrounding the unit-LAZ as the main factor to explain the accelerated etching rate in the lateral dimension near the unit-LAZ. Induced stress fields near and within the LAZ patterns can be significantly perturbed near the substrate surface. Different etched patterns can therefore be expected in the near sub-surface region from the etched features within the bulk.

From the tunnel experiments (paragraph 3.1), we conclude that the etching rate is substantially faster along the central region of the LAZ. This is particularly visible in Fig. 2 (left side) and Fig. 3. An etching rate of typically 5 μm/min was measured in an HF solution of 5%.

Channels made of multiple laser-written lines show what seem to be different regimes depending of the pulse energy:

- For lower pulse energy (typically below 270 nJ), regular structures are found that have a spatial distribution similar to the lines in the exposed pattern. Differences of contrast in SEM observation indicate that a denser material is present in the central region of the LAZ. For instance, on Fig. 9, this region is about 400 nm wide for a half a μm line spacing. A well-defined interface is clearly visible between darker regions and a 100 nm-zone present in between. For power below 55 nJ, channels are barely etched after two hours etching in HF 2.5 %.
- For higher pulse energy (starting around 400 nJ), the etching is significantly inhomogeneous across the channels. Un-etched material remains in the center of the channels and tends to be larger in volume as the writing energy increases. This etched material displays a much more irregular and chaotic surface morphology. A distribution of holes ranging in size from 10 to 100 nm in diameter are observed (Fig. 8). Porosity as such may have resulted from micro-explosions and/or plasma shockwaves leave behind micro-cavities which are exposed as the etching progresses. This pitting of the surfaces is seen at the bottom of the channel written with pulse energies of 270nJ where, unlike at higher energies, the channel is completely etched out. Also noted is the apparent decrease in the number and size of these holes at the highest pulse energies.

It has been well accepted that amorphous silica contains ring structures with different sizes. From various theoretical models, it is widely believed that the structure of a-SiO_2 is a network of SiO_4 tetrahedra containing a wide distribution of irregular rings of order n ($2 \leq n \leq 6$, where n is the number of Si atoms in the ring) [12]. Computer simulation indicates that rings of order 5 and 6 are most commonly in a-SiO_2 [12].

We propose the following phenomenological model to interpret our experimental results:

- For energy levels below 270nJ, the fs-laser induces local compaction. The region affected is typically 400 nm wide for a line density of half a μm. To accommodate the strain induced by the volume reduction, a stress field is present and gradually decreases over several μm depending on the extent of the compacted region. C. Fiori *et al.* [13] have shown that for a-SiO_2 excimer irradiated specimen, the number of defects detected during compaction was too small for one to argue that the volume changes observed are due to defect creation alone. They concluded that the process of compaction in a-SiO_2 corresponds to the volume reduction found among the allotropic forms of crystalline-silica (c-SiO_2) with decreasing mean

#4156- $15.00 US Received 2 April 2004; revised 29 April 2004; accepted 30 April 2004

coordination of the planar rings. Furthermore, C. Fiori *et al.* [13] have also shown the evidence of wide continuum of polymorphs in a-SiO_2. These structural modifications disappear after annealing at 950C. Similarly, we have observed that waveguides written at pulse energies below 80 nJ are no longer seen after annealing at 600C for several hours [9].
We assume that the same compaction mechanism take place in specimen irradiated with fs-laser. As the ring order decreases, the Si – O – Si angle decreases and would increase the etching rate as it was shown by Agarwal *et al*. [5]. This would explain why the optimum etching rate is obtained for an energy level corresponding to the boundary between the two etching regime. At this optimal level, the distribution of low order ring would be the highest and therefore the more favorable for etching. Si – O – Si bond angle deformation may also occur through induced stress from near by compacted regions.

- It is clear that the densification of SiO_2 cannot continue beyond the limit of two-membered rings [14]. Therefore, once the energy level reaches the threshold where no more compaction is possible, ablation or irreversible damage occurs which would explain the presence of craters and voids observed for energy level higher than 135nJ. Adjacent ablated zones may induce a relaxation of the internal stress in the central portion of the channel. Therefore, according this model, this region would not be as susceptible to etching. However, edges were the internal stress (or stress gradient) can still be present would be preferentially etched.

5. Conclusions and Summary

We have presented a method suitable to manufacture in fused silica microfluidic channels of arbitrary shape and dimension. The process is based on the use of femtosecond laser irradiation, followed by chemical etching. A volume sampling method is used to expose the desired pattern prior to etching. Using mainly SEM observations, we have investigated the microstructures of partially or fully etched channels made with various laser parameters.
We conclude that:

- Etching is faster in the central portion of the laser track. Selectivity of 1:100 was found.
- Depending on the pulse energy level, the affected zone in term of etching selectivity can extend over a distance that is several times larger than the laser track.
- We suspect two mechanisms to be mainly responsible of the increase-etching rate: one is driven by the presence of internal stress and the second one by an average ring size reduction indicative of higher SiO_2 polymorphs in the laser track.

From these observations, we propose a phenomenological model to explain the fs-laser exposure that leads to the change in the etching rate. There are two regimes of etching. For pulse energies that are below 270 nJ, compaction is induced in a small volume (typ. 400 nm wide) centered on the laser trace. As ring order decreases, the Si – O – Si angle decreases. As a consequence, etching rate increases significantly. Furthermore, the compaction induces internal stress that relaxes over a typical range of a μm to a few μm. At higher level of energy, ablation starts occurring and porosity is found in the material and tends to relax the stress when adjacent tracks are present. Therefore, the structural change induced is less favorable to etching and no increase of etching rate is found with the exception of edges corresponding to the interface between laser-exposed and non-exposed material. At this interface, internal stress is present in the near by bulk material.

Acknowledgments

Parts of this work were funded by the New York State Office for Science, Technology and Academic Research (NYSTAR) and by the US Army Tacom National Automotive Center under grant DAAE07-03-C-L048.

#4156- $15.00 US Received 2 April 2004; revised 29 April 2004; accepted 30 April 2004